17th International Drying Symposium (IDS 2010)
Magdeburg, Germany, 3-6 October 2010

MODELING AND ENERGY EFFICIENCY OPTIMIZATION OF A LOW TEMPERATURE ADSORPTION BASED FOOD DRYER

J.C. Atuonwu[1], G. van Straten[1], H.C. van Deventer[2], A.J.B. van Boxtel[1]

[1]Systems and Control Group, Wageningen University, Netherlands
Tel.:+31 317483364, E-mail: james.atuonwu@wur.nl; gerrit.vanstraten@wur.nl; ton.vanboxtel@wur.nl

[2]TNO Quality of Life, Zeist, Netherlands
Tel.:+ +31 30- 694 4363, E-mail: henk.vandeventer@tno.nl

Abstract: A simulation model for energy consumption sensitivity analysis is developed for an adsorption dryer utilizing the released heat of adsorption for drying. The system is optimized with respect to the regeneration air inlet temperature, ratio of adsorbent to drying air flowrate and ratio of regeneration air to adsorbent flowrate. The exhaust streams of the process under these optimal operating conditions are analyzed for sensible and latent heat recovery potentials. Using zeolite as adsorbent, it is shown that by proper selection of the optimization variables and recovery of stream energies, the system's energy performance for low drying temperatures is improved considerably.

Keywords: modelling and simulation, adsorption drying, energy efficiency, process optimization, heat recovery

INTRODUCTION

Drying is an important unit operation applied in a wide variety of industries ranging from the food and agricultural to the pharmaceutical, pulp and paper, wood, mineral processing, textile and a host of others.. It is an energy intensive process that accounts for as much as 15% of industrial energy consumption (Kemp, 2005). Usually one of the last steps in food processing operations, drying conditions have significant effects on product quality. The development of energy efficient and product friendly dryers is thus an important issue in the food industry. Thermal efficiency, the most important index of dryer energy performance, is defined as the ratio of the energy required to evaporate water from the product to the total energy input of the dryer (Kudra, 2004). This is mathematically represented as,

$$\eta = \frac{Q_{vout}}{Q_{in}} \tag{1}$$

Hence, for convective dryers which constitute over 85% of all industrial dryers (Mujumdar, 2007), the drying capacity essentially Q_{vout}, can be improved by increasing the quantity of moisture evaporated under the same throughput conditions. This can be achieved by raising drying air temperature, reducing its absolute humidity or a combination of both (Djaeni, et al., 2007(a)). For the same drying capacity, efficiency can be improved by reducing the effective energy input through heat recovery procedures as seen in (2)

$$\eta_{eff} = \frac{Q_{vout}}{Q_{in} - Q_{rec}} \tag{2}$$

Due to the limiting effect of high drying temperatures on the retention of nutritive components in food materials (Ratti, 2001), low and medium temperature drying have been proposed for such materials.

Drying air dehumidification using adsorbents leads to a reduction in absolute humidity accompanied by the release of adsorption heat (Djaeni et al., 2007(b); Gurtas and Evranuz, 2000). The combined effect increases the drying capacity of the air without raising the temperatures to undesirable high values. The limitation of this approach however lies in the energy required to regenerate the spent adsorbent. For instance, Madhiyanon et al. (2007) in an experimental study on a silica gel-based adsorption dryer report a 30-35% improvement in drying capacity but with a 40-80% increase in energy expenditure as a result of regenerating at a temperature of $101\,^{\circ}C$. Djaeni et al. (2007(a)) carried out simulation studies on a zeolite system with a regeneration temperature of $300\,^{\circ}C$. Although an improvement in drying capacity was recorded, the high regeneration temperatures used for the chosen zeolite, air and product flowrates more than negated

the improvement. The result for a single-stage system without heat recovery was a system efficiency of 48.6%. Although multistaging and heat recovery were proposed and implemented for improved efficiency, these come at extra capital costs. Moreover, the possibility of improving system performance prior to heat recovery by the optimal choice of operating conditions was not explored. In these studies, the determination of the free parameters of the system such as the regeneration temperature, regeneration air and adsorbent flowrates was based on engineering judgment and throughput considerations alone. No energy efficiency-based optimization procedure was applied.

Process optimization provides a means of driving processes to operate at the best possible point with regard to specific objective(s) while respecting defined constraints. To achieve this, models capable of reliable sensitivity analysis of the objective function with respect to the decision variables are required. Many mathematical models are available in literature for the simulation of the operation of various categories of adsorbent and drying systems each, considered in isolation. Although both processes are well-understood, very few models are available that show systematically, the interactions between them and how system energy efficiency is affected. Those available are either too complex for fast online optimization as in the case of the CFD formulation proposed by Djaeni et al. (2008) or lack the necessary level of detail for reliable optimization. In the latter case, simplifying assumptions which are infeasible in actual operational situations are usually made. For instance zero moisture content of sorbent at adsorber inlet and saturation at outlet without considering sorption equilibria and kinetics, 90% moisture removal from air at adsorber, 40% relative humidity of air at dryer exit, equal temperatures of solid and vapour phases in the adsorption and dryer subsystems are assumed in (Djaeni et al., 2007(a); Djaeni et al., 2007(b))). This tends to limit the freedom of the system to respond to changes in free variables. Moreover, product drying kinetics was not taken into consideration even though this has strong effects on drying rate and hence efficiency as well as product heating which ultimately will affect quality.

In this work, a generalized model for the simulation of the continuous operation of an adsorption dryer is developed without making the prior listed assumptions. An interesting feature of the model is the unified manner in which the adsorber, regenerator and dryer equations are presented in matrix form. The model which considers the drying kinetics of a specific food product (figs), (El-Sebaii, et al., 2002) is simple but detailed enough for reliable optimization. The energy efficiency of the system is optimized subject to temperature and moisture constraints on the product which indicate quality. Furthermore, sensible and latent heat recovery from

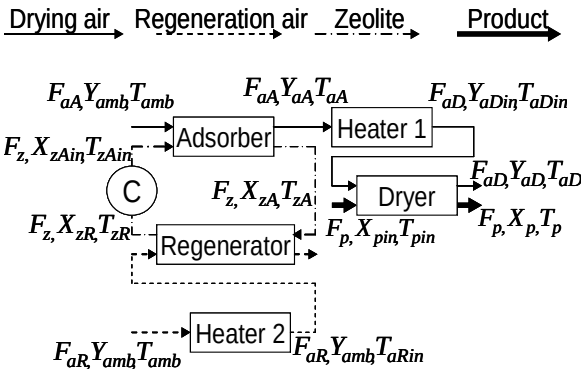

Fig. 1. Drying system process configuration where C stands for Cooler

the exhaust streams of the optimized process is investigated.

PROCESS DESCRIPTION

The process consists of the dryer, heat sources and a zeolite adsorption and regeneration system. Ambient air is passed through a zeolite bed where it undergoes dehumidification. It is then heated (where necessary) in Heater 1 to the desired drying temperature (Fig. 1), after which it is used for drying. Meanwhile, the spent zeolite is regenerated using hot air obtained by passing ambient air through Heater 2. The zeolite circulates alternately between the adsorber and the regenerator.

MODEL FORMULATION

The model is formulated on the following assumptions:

- Each of the phases in each subsystem is well-mixed so that the system can be approximated by a lumped parameter model
- Thermodynamic properties of the solid and fluid phases are constant
- Hysteresis between adsorption and desorption isotherms for the zeolite system is neglected
- Heat of sorption of the zeolite system is constant
- Thin layer drying is assumed so the drying process is governed by first-order kinetics

Mathematical model

The unified mass and energy balances governing the dynamic behaviour of the dryer, adsorber and regenerator subsystems are given by the ordinary differential equations

$$\frac{d\mathbf{Y_a}}{dt} = \frac{\mathbf{F_a}}{\rho_a \mathbf{V_a}}\left(\mathbf{Y_{ain}} - \mathbf{Y_a}\right) + \frac{\mathbf{k}\rho_s \mathbf{V_s}}{\rho_a \mathbf{V_a}}\left(\mathbf{X} - \mathbf{X_e}\right) \tag{3}$$

$$\frac{d\mathbf{T_a}}{dt} = \frac{\mathbf{F_a}}{\rho_a \mathbf{V_a} C_{pa}}\left[\begin{array}{l}\left(C_{pa} + \mathbf{Y_{ain}} C_{pv}\right)\mathbf{T_{ain}} \\ -\left(C_{pa} + \mathbf{Y_a} C_{pv}\right)\mathbf{T_a} + \\ \left(\mathbf{Y_{ain}} - \mathbf{Y_a}\right)\Delta H_v\end{array}\right] - \frac{\mathbf{h V_s}\left(\mathbf{T_a} - \mathbf{T_s}\right)}{\rho_a \mathbf{V_a} C_{pa}} \tag{4}$$

$$\frac{d\mathbf{X_s}}{dt} = \frac{\mathbf{F_s}}{\boldsymbol{\rho}_\mathbf{s}\mathbf{V_s}}\left(\mathbf{X_{sin}} - \mathbf{X_s}\right) - \mathbf{k}\left(\mathbf{X_s} - \mathbf{X_e}\right) \tag{5}$$

$$\frac{d\mathbf{T_s}}{dt} = \frac{\mathbf{F_s}}{\boldsymbol{\rho}_\mathbf{s}\mathbf{V_s}\mathbf{C_{ps}}}\left[\left(\mathbf{C_{ps}} + \mathbf{X_{sin}}C_{pw}\right)\mathbf{T_{sin}} - \left(\mathbf{C_{ps}} + \mathbf{X_s}C_{pw}\right)\mathbf{T_s}\right] - \frac{\mathbf{k}H_{ads}\boldsymbol{\zeta}\left(\mathbf{X_s} - \mathbf{X_e}\right)}{\mathbf{C_{ps}}} + \frac{\mathbf{h}\left(\mathbf{T_a} - \mathbf{T_s}\right)}{\boldsymbol{\rho}_\mathbf{s}\mathbf{C_{ps}}}. \tag{6}$$

where all divisions and products are element-wise and each "bold" term is a 3-dimensional vector in the form $\left[Dryer\ \ Adsorber\ \ \mathrm{Re}\,generator\right]$ such that

$$\begin{bmatrix}\mathbf{X_s}\\ \mathbf{Y_a}\\ \mathbf{T_a}\\ \mathbf{T_s}\end{bmatrix} = \begin{bmatrix}X_p & X_{zA} & X_{zR}\\ Y_{aD} & Y_{aA} & Y_{aR}\\ T_{aD} & T_{aA} & T_{aR}\\ T_p & T_{zA} & T_{zR}\end{bmatrix} \tag{7}$$

$$\begin{bmatrix}\mathbf{X_{sin}}\\ \mathbf{Y_{ain}}\\ \mathbf{T_{ain}}\\ \mathbf{T_{sin}}\\ \mathbf{F_a}\\ \mathbf{F_s}\end{bmatrix} = \begin{bmatrix}X_{pin} & X_{zAin} & X_{zRin}\\ Y_{aDin} & Y_{aAin} & Y_{aRin}\\ T_{aDin} & T_{aAin} & T_{aRin}\\ T_{pin} & T_{zAin} & T_{zRin}\\ F_{aD} & F_{aA} & F_{aR}\\ F_p & F_z & F_z\end{bmatrix} \tag{8}$$

$$\begin{bmatrix}\mathbf{C_{ps}}\\ \boldsymbol{\rho}_\mathbf{s}\\ \mathbf{V_s}\\ \mathbf{V_a}\end{bmatrix} = \begin{bmatrix}C_{pp} & C_{pz} & C_{pz}\\ \rho_p & \rho_z & \rho_z\\ V_p & V_{zA} & V_{zR}\\ V_{aD} & V_{aA} & V_{aR}\end{bmatrix} \tag{9}$$

and,

$$\begin{bmatrix}\mathbf{k}\\ \mathbf{X_e}\\ \mathbf{h}\end{bmatrix} = \begin{bmatrix}k_D & k_{zA} & k_{zR}\\ X_{pe} & X_{zeA} & X_{zeR}\\ h_D & h_{zA} & h_{zR}\end{bmatrix} \tag{10}$$

The vector $\boldsymbol{\zeta}$ is a "selection" vector that qualifies adsorption heat release/absorption. Since adsorption heat release/adsorption is highly significant only in the adsorber and regenerator,

$$\boldsymbol{\zeta} = \begin{bmatrix}0 & 1 & 1\end{bmatrix} \tag{11}$$

Constitutive Relations

For the zeolite system, a set of 2-dimensional vectors is defined

$$\begin{bmatrix}\mathbf{F_{az}} & \mathbf{G_{az}} & \mathbf{T_{az}} & \mathbf{Y_{az}} & \mathbf{T_{zz}} & \mathbf{X_{zz}} & \mathbf{X_{ze}} & \mathbf{k_z} & \mathbf{h_z} & \mathbf{P_v}\end{bmatrix} = \begin{bmatrix}F_{aA} & G_{aA} & T_{aA} & Y_{aA} & T_{zA} & X_{zA} & X_{eA} & k_{zA} & h_{zA} & P_{vA}\\ F_{aR} & G_{aR} & T_{aR} & Y_{aR} & T_{zR} & X_{zR} & X_{zeR} & k_{zR} & h_{zR} & P_{vR}\end{bmatrix} \tag{12}$$

The kinetic and equilibrium relations (Djaeni et al., 2008; van Boxtel et al., 2010) are

$$\mathbf{k_z} = k_0 \exp\left(-E_0/R\mathbf{T_{az}}\right) \tag{13}$$

$$\mathbf{X_{ze}} = \frac{X_{z\max}\mathbf{bP_v}}{1 + \mathbf{bP_v}} \tag{14}$$

$$\mathbf{b} = b_0 \exp\left(\frac{-E_1}{R\mathbf{T_{az}}}\right) \tag{15}$$

where the vapour pressure of the air is

$$\mathbf{P_v} = \frac{\mathbf{Y_{az}}P_{atm}}{0.62198 + \mathbf{Y_{az}}} \tag{16}$$

The volumetric heat transfer coefficient is determined from the Nusselt number correlation (Goncharov et al., 1975)

$$\mathbf{h_z} = \frac{\mathbf{Nu}\lambda_z}{{D_h}^2} \tag{17}$$

$$\mathbf{Nu} = 0.015\left(\mathbf{G_{az}}D_h/\mu_a\right)^{1.6} \tag{18}$$

The drying kinetics of figs (El-Sebaii, 2002) is used in evaluating the performance of the proposed system. The drying rate constant and equilibrium moisture content for this product are respectively:

$$k_D = -5.49x10^{-4} + 1.917x10^{-6}T_p \tag{19}$$

$$X_{pe} = \left(-\ln\left(1 - RH\right)/2.0108x10^{-2}T_p\right)^{1/1.1714} \tag{20}$$

where the relative humidity RH of the drying air is determined from ASHRAE (1997).

The volumetric heat transfer coefficient for air to product in the dryer is given from Sun et al. (1995) as

$$h_D = 3299\left(\frac{G_{aD}T_{aD}}{P_{atm}}\right)^{0.6011} \tag{21}$$

Coupling Equations

Based on the configuration of Fig. 1, the following are the coupling equations of the process

$$\begin{bmatrix}T_{aDin} & Y_{aDin}\end{bmatrix} = \begin{bmatrix}T_{aA} & Y_{aA}\end{bmatrix} \tag{22}$$

$$\begin{bmatrix}T_{aAin} & Y_{aAin} & X_{zAin}\\ T_{zRin} & Y_{aRin} & X_{zRin}\end{bmatrix} = \begin{bmatrix}T_{amb} & Y_{amb} & X_{zR}\\ T_{zA} & Y_{amb} & X_{zA}\end{bmatrix} \tag{23}$$

Forcing Signals and State Space Representation

The time-dependent external variables that affect the system can be derived from Fig. 1. They can be categorized in external inputs $\mathbf{d}$ and control inputs $\mathbf{u}$. The external inputs are

$$\mathbf{d} = \begin{bmatrix}T_{amb} & Y_{amb} & X_{pin} & T_{pin} & F_p\end{bmatrix}^T \tag{24}$$

With only Heater 2 in place, the control inputs in the current scheme are

$$\mathbf{u} = \begin{bmatrix} F_{aA} & F_{aR} & F_z & T_{aRin} & T_{zAin} \end{bmatrix}^T \quad (25)$$

The throughput is not taken as a control input, but rather as an external signal on the premise that a specific throughput is desired.

The system states (from (3) to (7)) are

$$\mathbf{x} = \begin{bmatrix} X_p & X_{zA} & X_{zR} & Y_{aD} & Y_{aA} & Y_{aR} & T_{aD} & T_{aA} & T_{aR} & T_p & T_{zA} & T_{zR} \end{bmatrix}^T \quad (26)$$

With these definitions, the system can be represented concisely in state space form as

$$\frac{d\mathbf{x}}{dt} = \mathbf{f}(\mathbf{x}, \mathbf{u}, \mathbf{d}, p) \quad (27)$$

Where $\mathbf{f}$ is a vector valued function with the same dimension as $\mathbf{x}$ that follows from (3) – (26), and p is a set of parameters as defined in Appendix 1.

Degrees of Freedom and Steady State Model Solution

By setting the time derivatives to zero, the following steady-states are derived

$$\mathbf{X_s} = \frac{\mathbf{X_{sin}} + \mathbf{k X_e \rho_s V_s / F_s}}{1 + \mathbf{k \rho_s V_s / F_s}} \quad (28)$$

$$\mathbf{Y_a} = \mathbf{Y_{ain}} + \frac{\mathbf{k \rho_s V_s}}{\mathbf{F_a}} (\mathbf{X_s} - \mathbf{X_e}) \quad (29)$$

$$\mathbf{T_a} = \frac{\mathbf{AB} + \mathbf{CD}}{\mathbf{AE} - \mathbf{C^2}} \quad (30)$$

where,

$$\mathbf{A} = \mathbf{F_s}(\mathbf{C_{ps}} + \mathbf{X_s} C_{pw}) + \mathbf{h V_s} \quad (31)$$

$$\mathbf{B} = \mathbf{F_a}\left[(C_{pa} + \mathbf{Y_{ain}} C_{pv})\mathbf{T_{ain}} + (\mathbf{Y_{ain}} - \mathbf{Y_a})\Delta H_v\right] \quad (32)$$

$$\mathbf{C} = \mathbf{h V_s} \quad (33)$$

$$\mathbf{D} = \mathbf{F_s}(\mathbf{C_{ps}} + \mathbf{X_{sin}} C_{pw})\mathbf{T_{sin}} - \mathbf{k} H_{ads} \boldsymbol{\rho_s} \mathbf{V_s} \zeta (\mathbf{X_s} - \mathbf{X_e}) \quad (34)$$

$$\mathbf{E} = \mathbf{F_a}(C_{pa} + \mathbf{Y_a} C_{pv}) + \mathbf{h V_s} \quad (35)$$

$$\mathbf{T_s} = \frac{\mathbf{F_s}\left[(\mathbf{C_{ps}} + \mathbf{X_{sin}} C_{pw})\mathbf{T_{sin}}\right] - \mathbf{k H_{ads}} \boldsymbol{\rho_s} \mathbf{V_s} \zeta (\mathbf{X_s} - \mathbf{X_e}) + \mathbf{h V_s T_a}}{\mathbf{F_s}(\mathbf{C_{ps}} + \mathbf{X_s} C_{pw}) + \mathbf{h V_s}} \quad (36)$$

To solve the system, the number of unknowns must be equal to the number of equations. As there are 12 state equations in 22 variables (12 states and 10 inputs), any set of the 10 variables out of 22 can be chosen to solve for the remaining 12.

The system of equations is highly coupled such that for zero degree of freedom an analytical solution is not possible. For instance as seen in (30) – (36), the steady-state values of the air, product and sorbent temperatures depend on the values of their moisture contents. These in turn depend on the sorption properties (see (28) – (29)) which are again, functions of the temperatures (see (13) – (14) & (19) – (20)). Similarly, the adsorber-regenerator zeolite loop requires the specification of the inlet moisture content to the adsorber X_{zAin}. This however must match the value of the moisture content X_{zR} (23) from the regenerator for which prior knowledge is unavailable. We thus have an algebraically looped system for which there is no analytical solution. Fig. 2 shows an iterative procedure applied to solve this problem. Here, all the input variables $\mathbf{d}$ and $\mathbf{u}$ are chosen as fixed. First of all, the coupled variables, e.g. T_{aA} and Y_{aA} are guessed and then, substituted into the relevant equations to obtain X_{ze}, X_{zA}, T_{zA}, T_{aA} and Y_{aA}. The calculated values are compared with the guessed values. The absolute value of the difference forms the basis of the decision in the next step. If this difference is less than some specified tolerance, the iteration stops; otherwise, the iteration continues with the next guess value modified by making it a weighted sum of the previous guess and the calculated value. The weighting factor ψ is a damping factor $0 < \psi < 1$ that determines the speed and stability of convergence. High values of ψ mean a more conservative approach for which convergence is slower but with low tendency to numerical instability. For low values, the system is more prone to numerical instability. For the current case, a ψ value of 0.8 is chosen and found good for the stability and fast convergence of the entire system.

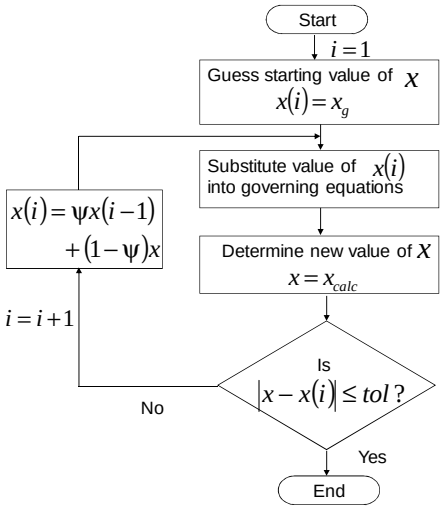

Fig. 2. Model solution algorithm

OPTIMIZATION PROBLEM FORMULATION

First of all, the following outputs that are important from the perspective of energy efficiency are defined. The instantaneous energy rate associated with the removed water is given by

$$Q_{vout} = F_p\left(X_{pin} - X_p\right)\Delta H_v \tag{37}$$

Similarly, for Heater 2 disabled (to limit drying temperatures), the instantaneous input energy rate is

$$Q_{in} = F_{aR}\left(C_{pa} + Y_{aRin}C_{pv}\right)\left(T_{aRin} - T_{amb}\right) \tag{38}$$

The total energy associated with these terms over time t is given by $\int_0^t Q_{vout}dt$ and $\int_0^t Q_{in}dt$ respectively. For steady-state optimization (see Fig.1.), it is assumed that of the 10 free inputs, $F_p, T_{amb}, Y_{amb}, T_{pin}, X_{pin}$ are fixed. Of the remaining 5, T_{zAin} is chosen to be equal to ambient temperature for which the cooler C is to be appropriately rated. For a given dryer size, F_{aA} is fixed. The remaining three F_z, F_{aR}, T_{aRin} can be chosen as optimization variables. For a given drying air flow, an optimal flow of zeolite is required, and for this, an optimal flow of regeneration air is needed. Hence, operational design variables r_1, r_2 are defined as:

$$F_z = r_1 F_{aA} \tag{39}$$

$$F_{aR} = r_2 F_z \tag{40}$$

The ratios r_1 and r_2 are chosen as optimization variables in addition to T_{aRin}. Hence, the optimization problem is formulated as

Maximize

$$\eta_U = \frac{Q_{vout}}{Q_{in}} = \frac{F_p\left(X_{pin} - X_{pout}\right)\Delta H_v}{F_{aR}\left(C_{pa} + Y_{aRin}C_{pv}\right)\left(T_{aR} - T_{amb}\right)} \tag{41}$$

where

$$U = \begin{bmatrix} T_{aRin} & r_1 & r_2 \end{bmatrix} \tag{42}$$

subject to (7 – 36), and the constraints

$$X_p = 0.05 \tag{43}$$

$$T_p \le 50 \tag{44}$$

$$U_{\min} \le U \le U_{\max} \tag{45}$$

OPTIMIZATION RESULTS AND DISCUSSION

The optimization was performed at different starting points and bounds on the decision variables. The results are summarized thus:

- The optimization results are independent of the starting points of each decision variable, suggesting that there are no local minima.
- The results are independent of the magnitudes of the lower bound on each decision variable, implying that they are not limiting.
- The results are also independent of upper bounds on the decision variables except the regeneration air inlet temperature. A significance of this upper bound is that above $400\,^{\circ}C$ (van Boxtel et al., 2010), the zeolite undergoes deformation so that the kinetic relations presented no longer hold.
- The optimal value of the regeneration air inlet temperature equals its upper bound. Fig. 3 shows the variation of the optimization results with the upper bound on regeneration air inlet temperature. From the figure it is seen that the optimal value varies linearly (with unit slope) as the upper bound. This is attributable to the fact that at higher regeneration temperatures, the zeolite going into the adsorber has a higher adsorption capacity (after cooling). It therefore should enhance greater reduction in the humidity of the drying air, and hence increase drying capacity. However, since the drying capacity of the dryer is constrained to be constant (see (37) and (43)), the zeolite flow required for this drying capacity is reduced. As a result, the flow of regeneration air required for this reduced zeolite flow also reduces more than proportionately. The resultant effect of these system interactions is that the product $F_{aR}T_{aRin}$ in the objective function reduces progressively.
- The optimal value of energy efficiency increases with regeneration temperature. For drying of figs, the efficiency rises from 40.02% for $U = \begin{bmatrix} 150 & 0.0740 & 3.2730 \end{bmatrix}$, to 68.76% for $U = \begin{bmatrix} 400 & 0.0237 & 1.9802 \end{bmatrix}$. An Efficiency of 68.76% is achieved. This is a significant improvement over previous results (Djaeni et al., 2007(a)) where an equivalent single-stage adsorption dryer without heat recovery recorded an efficiency of 48.6% while a conventional dryer operating at higher temperatures was 63.6% efficient.
- High regeneration temperatures are not a disadvantage if the corresponding air and zeolite flows are systematically optimized.
- The high energy contents of the zeolite and air from the regenerator creates opportunities for heat recovery which could further increase energy efficiency.

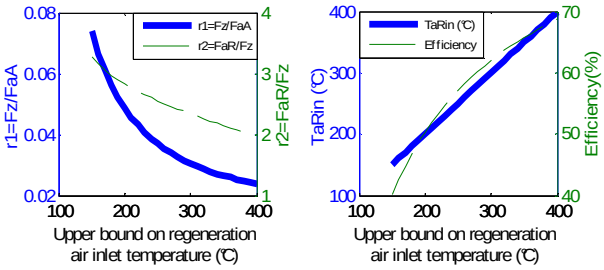

Fig. 3. Variation of optimization results with upper bound on regeneration inlet temperature

ENERGY RECOVERY

To fully exploit the energies of the system, heat recovery is essential. Pinch analysis is a targeting procedure that gives an indication of the maximum energy recoverable from a given process. The drying system under study has two main “hot streams”, the regenerator outlet air and zeolite and one “cold stream”, the ambient air to the regenerator. Kemp (2007) shows a simplified tabular method of determining the pinch. In this approach, the cold stream temperatures are shifted upwards by one-half the minimum exchanger temperature difference $\Delta T_{\min}$ while those of the hot streams are reduced by the same value (see Figs. 4, 5 & 6 as well as Table 1). Heat exchange is then calculated on each shifted temperature interval Δi. Traditionally, latent heat recovery is not considered. In order to investigate the possibilities for latent heat recovery, the dew-point of the air streams is an important variable of interest. This is because, when a moist air stream is cooled below its dew-point, latent heat can be recovered. For the regenerator output air, the dew point T_{dptR} is calculated by finding the value of the dry bulb temperature T_{aR} at which the relative humidity is unity, absolute humidity remaining constant. The optimization results show that as the optimal

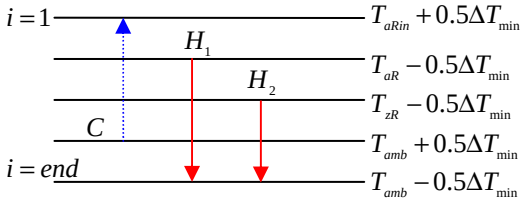

Fig. 4. Grid diagram showing heat recovery possibilities for Case 1: $T_{dptR} < T_{amb}$

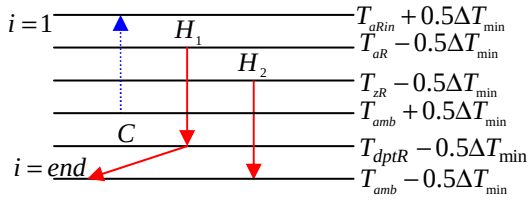

Fig. 5. Grid diagram showing heat recovery possibilities for Case 2: $T_{amb} < T_{dptR} < T_{amb} + \Delta T_{\min}$

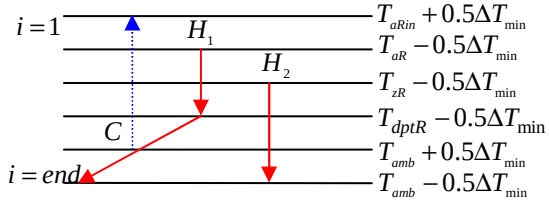

Fig. 6. Grid diagram showing heat recovery possibilities for Case 3: $T_{dptR} > T_{amb} + \Delta T_{\min}$

regeneration inlet air temperature T_{aRin} increases, the dew point of the exhaust rises. Thus, for some values of T_{aRin}, the dew point of the exhaust T_{aR} becomes higher than the intended discharge temperature (the ambient value). This means there are opportunities for latent heat recovery by cooling below the dew point. For other cases, the dew point is less, hence, no possibility of latent heat recovery. This situation gives rise to the three scenarios shown in Figs. 5, 6 & 7. In Case 1, there is no possibility of latent heat recovery as this covers cases where the dew point temperature of H1 is less than the target values. For Cases 2 and 3, the dew point is higher than the target value; hence theoretically, latent heat is recoverable. However, because of the minimum temperature difference needed for operation, Case 2 which covers situations where $T_{dptR} < T_{amb} + \Delta T_{\min}$ becomes such that latent heat is not recoverable. In Case 3 where $T_{dptR} > T_{amb} + \Delta T_{\min}$, latent heat recovery is possible. The inclined lines show the latent heat recovery paths for each interval while the vertical lines show sensible heat recovery. For each temperature (energy) interval Δi, the maximum sensible and latent heat recovery (Q_{sens} and Q_{lat}) are calculated using the formulae shown in Table 2.

Energy Recovery Results and Discussion

Fig. 7 shows the evolution of exhaust temperatures of zeolite and air from the regenerator under optimal conditions as well as the dew point of the exhaust air. The corresponding sensible heat and latent heat recovery obtained by performing calculations based on Tables 1 and 2 are also shown. It is seen that for

Table 1. Determination of shifted stream temperatures and associated heat capacity rates

Stream type	Supply temperature T_s	Target temperature T_t
H1	T_{aR}	T_{amb}
H2	T_{zR}	$T_{zAin} = T_{amb}$
C2	T_{amb}	T_{aRin}
Stream type	Shifted supply temperature S_s	Shifted target temperature S_t
H1	$T_{aR} - 0.5\Delta T_{\min}$	$T_{amb} - 0.5\Delta T_{\min}$
H2	$T_{zR} - 0.5\Delta T_{\min}$	$T_{amb} - 0.5\Delta T_{\min}$
C2	$T_{amb} + 0.5\Delta T_{\min}$	$T_{aRin} - 0.5\Delta T_{\min}$

Table 2. Determination of sensible and latent heat recovery in each temperature interval

$Q_{sens}(\Delta i)$	$\left(\sum FC_{pH}(\Delta i) - \sum FC_{PC}(\Delta i)\right)\left(S(i) - S(1+i)\right)$
$Q_{lat}(\Delta i)$	$F_{aR}\Delta H_v\left(Y_{aR}(T_{aR}, RH=1) - Y_{aR}(T_{amb}, RH=1)\right)$

some low values of regenerating temperature, latent heat recovery is impossible. At high values, latent heat recovery increases until it approaches a saturation region. Also, due to the nonlinear input-output temperature characteristics of the regenerator, the percentage value of the sensible heat recovery relative to the energy requirement drops in spite of the increase in the exhaust temperature and hence, absolute sensible heat recovery. In all, the effective value of the overall efficiency (calculated from equation (2)) rises to a maximum value of 125% which is approximately twice the value without heat recovery (68.76%). Table 3 shows some relevant system energy flows obtained for the particular case where regeneration air inlet temperature is $400^\circ C$. The associated flowsheet indicating heat recovery loops using a condensing heat exchanger (Hex) is shown in Fig. 8 for a $2.9\times10^4\ kg/hr\ db$ drying air flowrate. Comparing our results to that of Djaeni et al., 2007(a) where an efficiency of 72% after heat recovery was recorded, a significant improvement is seen. Meanwhile, for an equivalent conventional dryer (Djaeni et al., 2007(a)), heat recovery yielded no appreciable improvement from the 63.6% obtained without recovery. Moreover in the current system, product temperature constraints are satisfied. Associated with this are product quality benefits.

CONCLUSIONS

A generalized model for the simulation of the operation of an adsorption dryer has been developed and optimized. The adsorption, regeneration and drying processes have been shown to be governed by similar equations, so, a unified set of matrix equations can be used in describing the system operation. A parameter vector ζ has been introduced

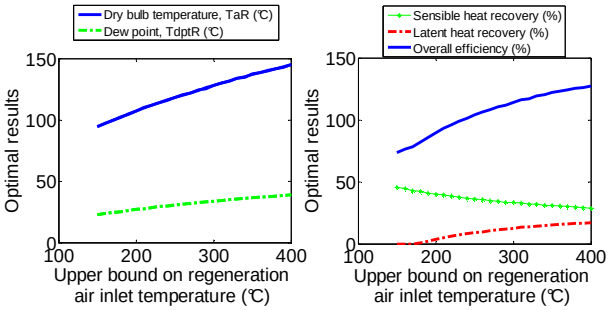

Fig. 7. Heat recovery possibility after optimization

Table 3. System energy flows for $T_{aRin} = 400^\circ C$

Total regeneration energy kJ/hr)	Evaporation energy (kJ/hr)	Sensible heat recovered (kJ/hr)	Latent heat recovered (kJ/hr)	η (%)
5.170×10^5	3.55×10^5	1.52×10^5	8.758×10^4	125

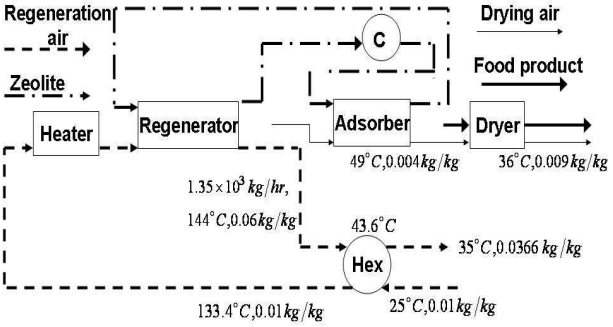

Fig. 8. Process flowsheet with heat recovery. Regeneration air dew point temperature $T_{dptR} = 43.6^\circ C$

which permits the same form of equations for the adsorber, dryer and regenerator. This vector accounts for the main difference in the energy balance which lies in the heat of adsorption.

The main results of the work are as follows:

- It has been shown that the energy and quality performance of a complex process such as adsorption drying can be formulated as an optimization problem. By optimizing the manner of energy consumption in the adsorber/regenerator system (with regeneration air inlet temperature, flowrate and zeolite flowrate as decision variables), the energy efficiency of the adsorption drying process under constrained drying conditions can be improved considerably.
- By applying efficient heat integration techniques (including latent heat recovery), to the optimized system, energy efficiency can be further increased to approximately twice the value without heat recovery.

ACKNOWLEDGEMENTS

This work is supported by the Energy Research Program EOS of the Dutch Ministry of Economics under Project EOSLTe7043.

NOMENCLATURE

b	Langmuir sorption constant	(–)
$\mathbf{C_p}$	Specific heat capacity	$Jkg^{-1}K^{-1}$
D_h	Hydraulic diameter	m
E	Kinetic parameters	$JKmol^{-1}$
ΔH	Latent heat of vaporization	Jkg^{-1}
$\mathbf{F}$	Mass flowrate	kgs^{-1}
$\mathbf{G}$	Mass flow per unit area	$kgm^{-2}s^{-1}$
h	Vol. heat transfer coefficient	$Wm^{-3}K^{-1}$
$\mathbf{k}$	Drying rate constant	s^{-1}
Nu	Nusselt number	(–)
P	Pressure	Pa
Q	Energy rate	Js^{-1}

R	Universal gas constant	$Jmol^{-1}K^{-1}$
r_1	Drying air/adsorbent flow	$kgkg^{-1}$
r_2	Ads./regeneration air flow	$kgkg^{-1}$
T	Temperature	K
tol	Tolerance	(–)
V	Volumetric hold up	m^3
X	Moisture content	$kgkg^{-1}\ db$
$X_{z\max}$	Adsorbent capacity	$kgkg^{-1}\,db$
Y	Absolute humidity	$kgkg^{-1}\,db$

Bold symbols refer to vectors given in equations 3-18 & 25-37

Greek letters

λ	Thermal conductivity	$Wm^{-1}K^{-1}$
μ	Viscosity	$kgm^{-1}s^{-1}$
ρ	Density	kgm^{-3}

Subscripts

a	Air	D	Dryer
A	Adsorber	dpt	Dew point
ads	Adsorption	e	Equilibrium
amb	Ambient	in, out	Input, output
atm	Atmospheric	p	Product
$calc$	Calculated	R	Regenerator
rec	Recovered	v	Vapour
sat	Saturation	w	Water
s	Solid	z	Zeolite

REFERENCES

ASHRAE (1997). Psychrometrics, *ASHRAE Fundamentals Handbook*, Atlanta, USA.

Boxtel, A.J.B. van., Boon, M.A., Deventer, H.C. and Bussmann, P.J. (*in press*). Zeolites for reducing drying energy usage, In: Tsotsas, E. and Mujumdar, A.S. (eds). *Modern Drying Technology Vol. 4: Energy Savings*, Wiley VCH.

Djaeni, M., Bartels, P.V., Sanders, J.P.M., Straten, G. van. and Boxtel, A.J.B. van (2007 (a)). Multistage zeolite drying for energy efficient drying. *Drying Technology, 25(6), 1053-1067*

Djaeni, M., Bartels, P.V., Sanders, J.P.M., Straten, G. van. and Boxtel, A.J.B. van (2007(b)). Process integration for food drying with air dehumidified by zeolites, *Drying Technology*, 25(1), 225-239

Djaeni, M., Bartels, P. V. Sanders, J. P. M., Straten, G. van. and Boxtel, A. J. B. van. (2008). Computational fluid dynamics for multistage adsorption dryer design, *Drying Technology*, 26(4), 487-502.

El-Sebaii, A.A., Aboul-Enein, S., Ramadan, M.R.I. and El-Gohary, H.G. (2002). Empirical correlations for drying kinetics of some fruits and vegetables, *Energy*, (27), 845-859.

Goncharov, V.V., Zavadovskii, E.G., Maikov, V.P., Sokolova, N.I., Solntsev, M.Y. and Yusova, G.M. (1975). Experimental determination of the volume coefficient of heat transfer from air to a granular bed of zeolite or silica gel. *Chemical and Petroleum* Engineering, 11(2), 127-130.

Gurtas, F. and Evranuz, Ö. (2000). Low temperature mushroom drying with desiccant dehumidifiers. *Drying Technology*, 18(1), 433-445.

Kemp, I.C. (2005). Reducing dryer energy use by process integration and pinch analysis, *Drying Technology*, 23(9), 2089-2104

Kemp, I.C. (2007). *Pinch Analysis and Process Integration: A User Guide on Process Integration for the Efficient Use of Energy*, Butterworth Heinemann.

Kudra, T. (2004). Energy aspects in drying. *Drying Technology 22(5), 917-932.*

Madhiyanon, T., Adirekrut, S., Sathitruangsak, P. and Soponronnarit, S. (2007). Integration of a rotary desiccant wheel into a hot-air drying system: Drying performance and product quality studies, *Chemical Engineering and Processing*, 46, 282-290.

Mujumdar, A.S. (2007). *Principles, classification and selection of dryers*. In: Handbook of Industrial Drying Technology, 3rd Edition, Mujumdar, A.S. (eds). Taylor and Francis Group

Ratti, C. (2001). Hot air and freeze-drying of high-value foods: a review. *Journal of Food Engineering*, 49, 311-319.

Sun, Y., Pantelides, C.C. and Chalabi, Z.S. (1995). Mathematical modeling and simulation of near-ambient grain drying. *Computers and Electronics in Agriculture*, 13(3), 243-271.

APPENDIX 1

Model parameters p

b_0	$5.62x10^{-8}$	E_0	$7.524x10^6$
C_{pa}	$1x10^3$	E_1	$-5.124x10^7$
C_{pv}	$1.93x10^3$	H_{ads}	$3.2x10^6$
C_{pw}	$4.18x10^3$	ΔH_v	$2.5x10^6$
C_{pz}	$8.36x10^2$	k_0	$4.04x10^{-2}$
D_h	$2x10^{-3}$	λ_z	0.15
R	$8.314x10^3$	μ_a	$1x10^{-3}$
ρ_a	1.2	P_{atm}	$1.01x10^5$
ρ_z	$1.2x10^3$	$X_{z\max}$	0.1896